SIZE OF CORONAL STRUCTURES IN ACTIVE STELLAR CORONAE FROM THE DETECTION OF X-RAY RESONANT SCATTERING

P. Testa[1,2], J. J. Drake[2], G. Peres[1] and E. E. DeLuca[2]

[1]Dip. Scienze Fisiche ed Astronomiche, Sezione di Astronomia, Università di Palermo, Piazza del Parlamento 1, 90134 Palermo, Italy
[2]Smithsonian Astrophysical Observatory, MS 3, 60 Garden Street, Cambridge, MA 02138

Abstract

We have analyzed high-resolution X-ray spectra of a large sample of active stars observed with the High Energy Transmission Grating Spectrometer on *Chandra* in order to investigate the properties of optical thickness of the coronal plasma. The analysis of Lyman series lines arising from hydrogen-like oxygen and neon ions shows in the coronae of the active RS CVn-type binaries II Peg and IM Peg significant decrements in the Lyα/Lyβ ratios as compared with theoretical predictions and with the same ratios observed in similar active binaries. We interpret these depletions in terms of resonance scattering of line photons out of the line-of-sight. These observations present the first strong evidence for this effect in active stellar coronae.

The net line photon loss implies a non-uniform and asymmetric surface distribution of emitting structures on these stars. Escape probability arguments imply typical line-of-sight sizes of the coronal structures that dominate the X-ray emission of 10^{10} cm at temperatures of 3×10^6 K and 10^8 cm at 10^7 K. These sizes are an order of magnitude larger than predicted by simple quasi-static coronal loop models, but are still very small compared to the several 10^{11} cm radii of the stars.

Key words: Radiative transfer — X-rays: stars — Stars: coronae — Stars: late type — Stars: structure

1. Introduction

The Sun is the only star for which we can presently image coronal X-ray emission, and in order to understand how coronae on other stars might be structured we must resort to indirect means. Information on the coronal structuring is generally obtained through the application of techniques like for instance the study of evolution of lightcurves during flares (e.g. Favata et al. 2000; Maggio et al. 2000; Reale et al. 2004), rotational modulation (e.g. Brickhouse et al. 2001; Marino et al. 2003), and study of density properties together with information on emission measure (e.g. Testa et al. 2004b; hereafter Paper I). Most of these analyses indicate that the emitting plasma is rather compact (scale height $\leq 0.5R_\star$) and localized at high latitude (see e.g. Schmitt & Favata 1999; Brickhouse et al. 2001; Testa et al. 2004a; Testa et al. 2004b); however presence of extended coronal plasma has been claimed by e.g., Chung et al. (2004) and Redfield et al. (2003).

The search for signs of quenching in strong lines through resonance scattering represents a further technique that offers potentially powerful diagnostics of the sizes of X-ray emitting regions. The escape probability of a photon emitted by a resonance line in a low density homogeneous plasma is in fact dependent on the line-of-sight path length through the plasma region. Provided the plasma density and the abundance fraction of the ion in question are known, in the regime where the plasma is only marginally thick the comparison of strong and weak lines subject to different scattering losses can yield an estimate of the typical emitting region path length.

Previous works addressed the study of strong resonance lines exploring the properties of optical thickness of coronal emission. Resonance scattering in the solar corona has been studied predominantly in the light of the strong ($gf = 2.66$) $2p^6\,{}^1S_0 \rightarrow 2p^5 3d\,{}^1P_1$ resonance line of Fe XVII at 15.02 Å as compared to nearby weaker Fe XVII lines, though with controversial results concerning whether optical depth effects were seen or not (Phillips et al. 1996; Phillips et al. 1997; Schmelz et al. 1997; Saba et al. 1999). In particular, Saba et al. (1999) review recent observational findings on the opacity inferred from the study of the bright iron resonance line at 15.02 Å and on the center-to-limb behaviour. Among other issues, Saba et al. (1999) address the discrepancy in the derived direction and magnitude of the center-to-limb trend they find (also in agreement with Schmelz et al. 1997), as compared to the findings of Phillips et al. (1996); Phillips et al. (1996) find that the effect of resonant scattering is decreasing from the disk center toward the solar limb, trend irreconcilable and totally opposite to the trend of optical depth found by Saba et al. (1999) and Schmelz et al. (1997).

Studies of the same transition seen in different stars observed at high resolution ($\lambda/\Delta\lambda \sim 1000$) by *Chandra* have also recently been presented by Phillips et al. (2001) and Ness et al. (2003). Both stellar studies fail to find evidence for significant optical depth in Fe XVII. In particular the large survey of stellar spectra analyzed by Ness et al. (2003) show that no firm results can be obtained from Fe lines.

Proc. 13th Cool Stars Workshop, Hamburg, 5–9 July 2004 (ESA SP-560, Jan. 2005, F. Favata, G. Hussain & B. Battrick eds.)

There are two problems with using the prominent Fe XVII soft X-ray complex for optical depth studies. Recently, it has been shown by Doron & Behar (2002) and Gu (2003) that the indirect processes of radiative recombination, dielectronic recombination, and resonance excitation involving the neighbouring charge states are important for understanding the relative strengths of Fe XVII–XX lines, thus there is still some considerable difficulty in reconciling theoretical and observed line strength ratios. Secondly, the coronae of active stars have been found to be Fe-poor by factors of up to 10 compared with a solar or local cosmic composition (see e.g. reviews by Drake 2003; Audard et al. 2003); in the case of stellar coronae, where only the very strongest spectral lines might be expected to undergo any significant resonance scattering, such abundance depletions also reduce the sensitivity of Fe lines as optical depth indicators. For coronal abundances typically found in RS CVn systems (e.g. Drake 2003; Audard et al. 2003), we expect resonant lines from the more abundant ions like oxygen and neon, to be more sensitive to resonant scattering processes than the resonant iron line. Such effect is shown in Figure 1.

Indeed, the spectral lines likely to exhibit the largest optical depths in the coronae of active stars are the Lyman α lines of hydrogen-like O and Ne–elements that are often seen to be enhanced relative to Fe (e.g., Drake et al. 2001; Audard et al. 2003; Huenemoerder et al. 2001).

Although up till now these attempts failed to find any evidence, observational evidences urge to search for effects of resonant scattering. For instance the increasing evidence of high densities ($n_e \sim 10^{12}$ cm^{-3}) widely present in active stellar coronae at temperatures of the order of 6–10 MK, as widely discussed in Testa et al. (2004b), suggests that scattering in strong lines is not unlikely.

We present here an analysis of the Lyα to Lyβ line strength ratios in a number of active stars observed with the High Energy Transmission Grating Spectrometer (HETGS) on board the *Chandra* X-ray Observatory (CXO). We will show that in the active binaries II Peg and IM Peg the Lyα, β lines of Ne and O are significantly quenched. We use inferred optical depths to make the first direct estimates of the dimensions of coronal structures in active stars.

2. Observations and analysis

Observations and relevant characteristics of the program stars are discussed in detail in Testa et al. (2004b); Table 1 summarizes the characteristics of a sub-sample of stars we are focusing on. All spectra were obtained by the *Chandra* HETGS in conjunction with the Advanced CCD Imaging System spectroscopic detector (ACIS-S), and were downloaded from the *Chandra* Data Archive[1]. Spectra from multiple observations (e.g., IM Peg and AR Lac) were combined, and positive and negative orders were summed, keeping HEG and MEG spectra separate. The same observations of HR 1099, II Peg and AR lac are described in more detail by Drake et al. (2001), Huenemoerder et al. (2001) and Huenemoerder et al. (2003), respectively.

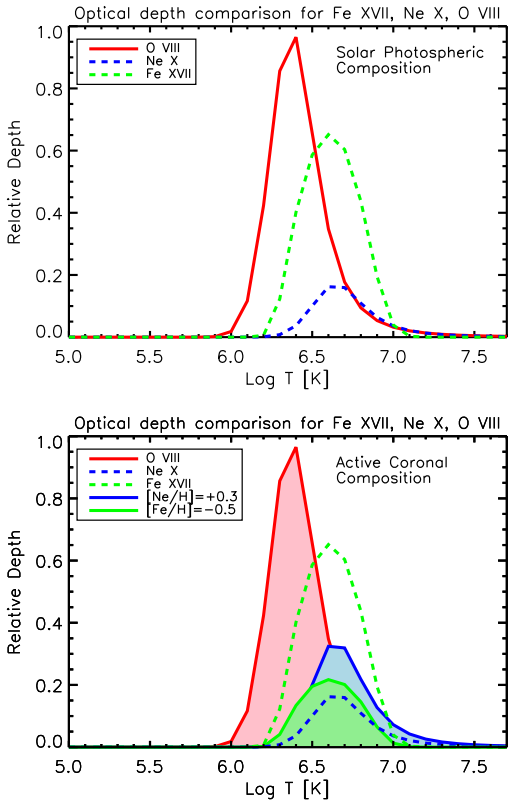

Figure 1. Sensitivity of Ne, O and Fe resonant lines to resonant scattering, assuming solar typical abundances (top) or coronal abundances typically found in RS CVn's (bottom; filled profiles). Because of the higher Ne abundance found in RS CVn systems (e.g. Audard et al. 2003), the expected resonant scattering is higher for O VIII and Ne X Lyα than for the Fe XVII resonance line at ~ 15.02 *Å.*

Resonance scattering of Lyα and Lyβ photons can be diagnosed by comparison of the measured Lyα/Lyβ ratio with respect to the theoretical ratio. Spectral line fluxes were measured using the FITLINES utility in the PINTofALE[2] IDL[3] software package (Kashyap & Drake 2000).

The Lyβ transition of O VIII is blended with an Fe XVIII line ($2s^2 2p^5\ ^2P_{3/2} - 2s^2 2p^4(^3P)3s\ ^2P_{3/2}$, $\lambda = 16.004$ Å). In order to take into account the effect of the blending, we estimated the intensity of this line by scaling the observed intensity of the neighbouring Fe XVIII 16.071 Å ($2s^2 2p^5\ ^2P_{3/2}-$

[1] http://cxc.harvard.edu/cda

[2] http://hea-www.harvard.edu/PINTofALE/

[3] Interactive Data Language, Research Systems Inc.

Table 1. Properties of observed stars and related HETG observations.

Source	Spectr. Type	d [a] [pc]	$R_\star/R_\odot$	$P_{\rm orb}$ [b] [ks]	$_P$rot [b] [ks]	$L_{\rm X}$ [A] HEG [erg/s]	$L_{\rm X}$ [A] MEG [erg/s]	$F_{\rm X}$ [B] [erg/cm^2/s]	Obs ID	$t_{\rm exp}$ [ks]
II Peg	K2V/..	42	3.4/.. [c]	580	580	$1.56{\cdot}10^{31}$	$1.76{\cdot}10^{31}$	$250\cdot10^5$	1451	42.7
IM Peg	K2III-II/..	96.8	13/.. [d]	2100	2100	$2.75{\cdot}10^{31}$	$2.79{\cdot}10^{31}$	$27.1\cdot10^5$	2527	24.6
IM Peg						$2.17{\cdot}10^{31}$	$2.30{\cdot}10^{31}$	$22.3\cdot10^5$	2528	24.8
IM Peg						$1.86{\cdot}10^{31}$	$1.97{\cdot}10^{31}$	$19.2\cdot10^5$	2529	24.8
AR Lac	G2IV/K0IV	42	1.8/3.1 [b]	170	170	$5.21{\cdot}10^{30}$	$5.60{\cdot}10^{30}$	$284\cdot10^5$	6	32.1
AR Lac						$5.61{\cdot}10^{30}$	$6.30{\cdot}10^{30}$	$319\cdot10^5$	9	32.2
HR 1099	G5IV/K1IV	29.0	1.3/3.9 [b]	250	250	$7.85{\cdot}10^{30}$	$1.05{\cdot}10^{31}$	$1020\cdot10^5$	62538	94.7

[A] HEG range: 1.5–15 Å; MEG range: 2–24 Å.
[B] X-ray surface flux from $L_{\rm X}$ obtained from MEG spectra
References: [a] SIMBAD database; [b] Strassmeier et al. (1993); [c] Berdyugina et al. (1998); [d] Berdyugina et al. (1999)

$2s^2 2p^4(^3P)3s\ ^4P_{5/2}$) transition, that shares the same upper level, by the ratio of their theoretical line strengths (0.76) as predicted by the APED database (Smith et al. 2001). Uncertainties involved in this deblending procedure are negligible for II Peg (whose Fe XVIII is weak) and similar to or less than Poisson errors for the other stars for, e.g., an error of $\sim 20\%$ in the theoretical Fe XVIII ratio. In order to take into account the slight dependence on temperature of the Lyα/Lyβ ratio, we also measured the He-like resonance lines of Ne IX and O VII, providing a temperature diagnostics from the Lyα/He-like r ratio. The line fluxes measured for all the lines, together with the statistical errors, are listed in Table 2.

Figure 2 shows a comparison of the observed Lyα/Lyβ ratios with the theoretical values for both O and Ne. The measured ratios are shown at the temperatures (listed in Table 3) at which observed H-like to He-like $2p$-$1s$ line intensities matched their theoretical (APED) values. It is worth noting that the temperature diagnostics based on the Lyα/He-like r ratio assumes that the lines are formed at a single temperature; however this approximation is not critical because the temperature dependences of these Lyα/Lyβ ratios are not steep for $T > 2$ MK. We note that, for all the considered sources, both O and Ne H-like lines are formed at temperatures significantly lower than those at which the theoretical Lyα/Lyβ ratios reach their asymptotic limits.

Figure 2 shows that the observed Lyα/Lyβ ratios are lower than the theoretical values for both the Ne X and the O VIII lines in the case of IM Peg, and for O VIII in II Peg. Huenemoerder et al. (2001) noticed similar discrepancies in II Peg but excluded optical depth effects on the grounds that this deviation was less than $\sim 2\sigma$ from the theoretical value; it appears, however, that this assessment was based on the high temperature asymptotic ratio of ~ 6.25 (in photon units). Taking into account the temperature effect, our measured ratio for II Peg is in-

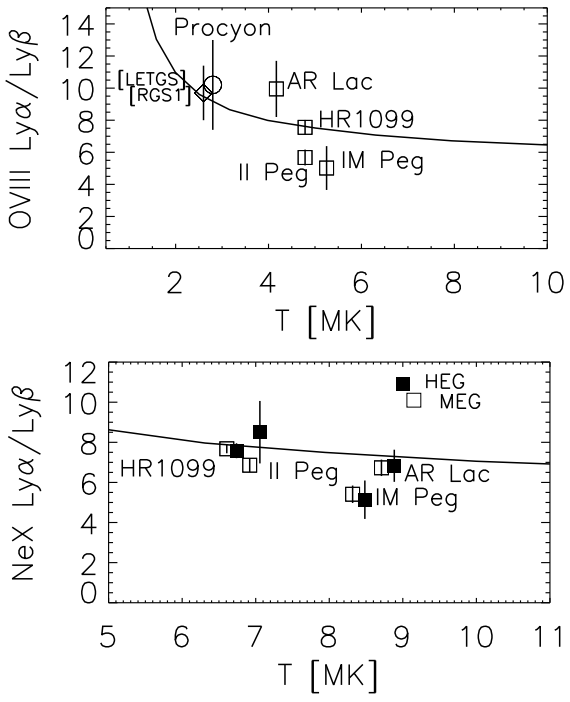

Figure 2. Lyα/Lyβ, both from HEG (filled symbols), and from MEG (empty symbols) vs. the temperature derived from the ratio of the Lyα and the resonance line of the He-like ion. The solid lines mark the theoretical ratio from APED, expected for isothermal plasma at the corresponding temperature. As indicated on the lower plot, different symbols are used for different classes of sources. Lyα/Lyβ ratios from HEG are shifted in T by 2% to distinguish them from the MEG measurements otherwise superimposed.

Table 2. Line flux measurements and Lyα/Lyβ ratios, with 1σ errors.

Source	grating	flux (10^{-6} photons cm^{-2} sec^{-1})							Photon Ratio	
		Ne X		Ne IX	O VIII		O VII	Fe XVIII	Lyα/Lyβ	
		Lyα 12.132Å	Lyβ 10.239Å	r 13.447Å	Lyα 18.967Å	Lyβ 16.006Å	r 21.602Å	16.071Å	Ne X	O VIII
II Peg	HEG	1364±70	160±28						8.5 ± 1.6	
	MEG	1217±28	178±8	365±21	2050±70	419±26	250±50	77±16	6.8 ± 0.3	5.6 ± 0.5
IM Peg	HEG	410±30	80±20						5.1 ± 0.9	
	MEG	385±13	71±2	77±11	530±40	145±22	52±25	55±13	5.4 ± 0.4	5.0 ± 1.2
AR Lac	HEG	727±30	106±11						6.8 ± 0.8	
	MEG	632±16	94±5	107±14	820±40	175±15	156±44	121±14	6.7 ± 0.4	9.9 ± 1.9
HR 1099	HEG	2180±40	288±13						7.6 ± 0.4	
	MEG	1705±21	222±6	571±16	2860±60	549±19	400±40	225±14	7.7 ± 0.2	7.6 ± 0.5

stead more than 3σ lower than the expected ratio at the temperature of formation of the O VIII lines. In the case of IM Peg, the observed O VIII ratio lies $\sim 1.8\sigma$ below the theoretical value, while the Ne X ratio in both HEG and MEG, are $> 3\sigma$ lower. For comparison with IM Peg and II Peg, we also present similar results for AR Lac and HR 1099: these active stars represent a valuable comparison since they show a very similar thermal structure but their Lyα/Lyβ ratios instead do not show significant departure from the expected optically thin values.

Though uncertainties in the theoretical ratio are not included, these are not expected to exceed 10% based on good agreement with recent laboratory experiments (G. Brown, private communication; Beiersdorfer 2003). If we assume a 10% error in theoretical ratios, the Ne Lyα/Lyβ of IM Peg still departs by 3σ for MEG ($\sim 1.7\sigma$ for HEG), while the O ratios lie 2.5σ for II Peg and 1.3σ for IM Peg below the theoretical curve. In Figure 2, we also plot the O VIII Lyα/Lyβ ratios obtained from the line fluxes measured by Raassen et al. (2002) from *Chandra*/LETGS and XMM-*Newton*/RGS1 spectra of Procyon. In the Procyon spectrum Fe XVIII is not detected and these data provide further validation of the APED O VIII Lyα/Lyβ ratio.

These quantitative results are reinforced by a visual comparison of spectra in Figure 3, in which the Lyα lines in II Peg and IM Peg are visibly weaker relative to Lyβ that those of AR Lac and HR 1099. There do not appear to be plausible explanations for the discrepant ratios other than by the quenching of Lyα relative to Lyβ through resonance scattering within the emitting plasma. Intervening photoelectric absorption could cause similar effects but H column densities of order a few 10^{21} cm^2 would be required–two or three orders of magnitude higher than inferred for these stars (Mewe et al. 1997; Mitrou et al. 1997).

Table 3. Plasma densities and temperatures.

Source	$\log n_e{}^{(A)}$		$\log T^{(B)}$	
	Mg XI	O VII	Ne	O
II Peg	$12.75^{+0.05}_{-0.25}$	$10.5^{+0.5}_{-0.25}$	6.85-6.9	6.65-6.75
IM Peg	$12.5^{+0.25}_{-0.25}$	-	6.9-6.95	6.65-6.85
AR Lac	< 12.25	-	6.9-7.0	6.6-6.7
HR 1099	$12.25^{+0.13}_{-0.13}$	$10.0^{+0.5}_{-0.7}$	6.75-6.8	6.67-6.7

[A] From He-like triplet diagnostics (Paper I).
[B] From Lyα/r ratio diagnostics.

2.1. Path length estimate

The measured line ratios, when compared with the expected values provide an effective optical depth τ, and a typical photon path length within the emitting plasma. We use the escape probability, $p(\tau)$, derived by Kastner & Kastner (1990), which for $\tau \leq 50$ can be approximated by (e.g. Kaastra & Mewe 1995):

$$p(\tau) \sim \frac{1}{1 + 0.43\ \tau} \qquad (1)$$

This is the escape probability for line photons emitted at optical depths between 0 and τ, averaged over a Gaussian line profile due to thermal Doppler broadening, and it assumes that each scattered photon is completely lost from the line of sight. This probability is significantly larger than the $e^{-\tau}$ transmittance of the simple absorption case, since it assumes emission over the whole line of sight through the plasma. The line center optical depth,

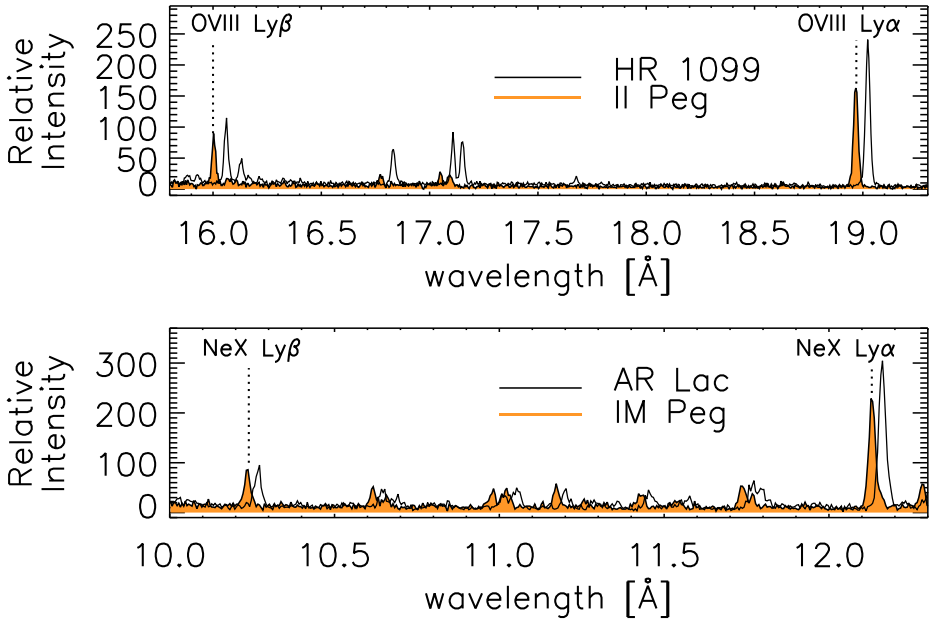

Figure 3. Comparison of the spectra for sources showing optical depth effects and sources appearing effectively optically thin. Top – O VIII *Lyα, β spectral region for II Peg (filled profile) and HR 1099 (shifted in λ by +0.06 Å for better readability). Spectra are normalized such that they have the same* unblended *Lyβ line strength, i.e. after correction for the Fe* XVIII *line flux (see text). The different strengths of the Fe line complex near 17 Å reflects primarily a different Fe/O abundance ratio in the two stars (Drake et al. 2001, Huenemoerder et al. 2001). Bottom – Ne* X *Lyα, β spectral region for IM Peg (filled spectrum) and AR Lac (shifted in λ by +0.03 Å for better readability). Spectra are again normalized to the observed intensities of the Lyβ line.*

τ, can be written (e.g., Acton 1978):

$$\tau = 1.16 \cdot 10^{-14} \cdot \frac{n_{\rm i}}{n_{\rm el}} A_{\rm Z} \frac{n_{\rm H}}{n_{\rm e}} \lambda f \sqrt{\frac{M}{T}} n_{\rm e} \ell \qquad (2)$$

for ion fraction $n_{\rm i}/n_{\rm el}$ (from Mazzotta et al. 1998), element abundance $A_{\rm Z}$, oscillator strength f, temperature T, electron density $n_{\rm e}$, atomic weight M, where $n_{\rm H}/n_{\rm e} \sim 0.85$, and ℓ is the total path length along the line of sight through the emitting plasma. In the above, neglect of non-thermal broadening should not be important: non-thermal velocities of, e.g., 50 km s^{-1} – similar to the thermal velocities for O and Ne at their characteristic temperatures of formation – would result in ℓ being underestimated by a factor of 1.4.

In order to derive an estimate of the photon path length we need an estimate of the electron densities and element abundances. We adopted the electron densities from the survey of Paper I, derived from the He-like triplet f/i density diagnostics. For τ(O VIII) we assumed the $n_{\rm e}$ derived from the O VII He-like triplet; the Ne IX triplet is strongly affected by blends with Fe lines and so for τ(Ne X) we assumed the $n_{\rm e}$ derived from the Mg XI He-like triplet that forms at a similar temperature. In the case of IM Peg, the low signal in the O VII intercombination and forbidden lines precludes a firm density estimate; we therefore assumed a value of 2×10^{10} cm^{-3}, which is typical of values obtained for all the measurable spectra of RS CVns in Paper I. The assumed $n_{\rm e}$ are listed in Table 3. As for the O and Ne abundances, for II Peg we assumed the coronal abundances derived by Huenemoerder et al. (2001). For IM Peg, since there is no available determination of coronal abundances, we adopted O and Ne coronal abundances scaling the values for II Peg (from Huenemoerder et al. 2001) by the ratio of II Peg to IM Peg photospheric metallicities, $[{\rm Fe/H}]_{\rm II} = -0.4$ and $[{\rm Fe/H}]_{\rm IM} = 0.0$, derived by Berdyugina et al. (1998,1999, respectively). The adopted abundances are listed in Table 4.

In order to derive an estimate of the path length, ℓ, we treated the fine structure components of Lyα (1: $^2P_{3/2} \rightarrow ^2S_{1/2}$ at $\lambda = 18.9671$ Å and 2: $^2P_{1/2} \rightarrow ^2S_{1/2}$ at $\lambda = 18.9726$ Å) separately, since their splitting ($\Delta\lambda/\lambda \sim 0.0003$) is larger than the thermal width ($\sim \sqrt{k_B T/M}/c \sim 0.00013$). The observed and theoretical intensities, $I_{\rm obs}$ and $I_{\rm th}$, are then related as follows:

Table 4. Path length derived from measured Lyα/Lyβ.

Source	Ion		Element [A] Abundance	ℓ_τ [cm]	$L_{\rm RTV}$ [B] [cm]	$\ell_\tau/L_{\rm RTV}$ [C]	$\ell_\tau/{\rm R}_\star$ [D]
II Peg	O VIII	MEG	8.97 [a]	$9.5\cdot10^9$	$1\cdot10^9$	~ 10	0.04
IM Peg	O VIII	MEG	9.37 [b]	$1.7\cdot10^{10}$	$2.2\cdot10^9$	~ 8	0.019
	Ne X	HEG	8.86 [b]	$1.6\cdot10^8$	$2.8\cdot10^7$	~ 6	0.0002
	Ne X	MEG		$2.2\cdot10^8$	$2.8\cdot10^7$	~ 8	0.00018

[A] Expressed on the usual spectroscopic logarithmic scale where X/H=log(n(X)/n(H))+12, and n(X) is the number density of the element X.
[B] Loop length from RTV scaling laws: $L_{\rm RTV}\sim T^2/[(1.4\cdot10^3)^3\cdot 2n_ek_B]$.
[C] Path length as fraction of the RTV loop length.
[D] Path length as fraction of the stellar radius.
[a] From Huenemoerder et al. (2001).
[b] Scaled from Huenemoerder et al. (2001) II Peg values by the ratio of II Peg to IM Peg photospheric metallicities, $[{\rm Fe/H}]_{\rm II}=-0.4$ and $[{\rm Fe/H}]_{\rm IM}=0.0$, derived by Berdyugina et al. (1998,1999, respectively).

$$I_{Ly\alpha\ \rm obs}=I_{1\ \rm obs}+I_{2\ \rm obs}=\frac{I_{1\ \rm th}}{1+0.43\tau_1}+\frac{I_{2\ \rm th}}{1+0.43\tau_2} \quad (3)$$

Since for hydrogenic ions $f_2=f_1/2=0.2776/2$ (e.g. Morton 2003), $I_{2\ \rm th}=I_{1\ \rm th}/2$, and $\tau_i\sim C(\ell)\cdot f_i$ (see Eq. 2), we obtain:

$$\frac{I_{Ly\alpha\ \rm obs}}{I_{Ly\alpha\ \rm th}}=\frac{1}{3}\left[\frac{2}{1+0.43C(\ell)f_1}+\frac{1}{1+0.43C(\ell)f_1/2}\right] \quad (4)$$

For Lyβ the splitting of the components is smaller than the thermal width and the escape probability for Lyβ is given directly by Eq. 1. The combined equation for $C(\ell)$ was then solved to obtain the path length.

The path length estimates, ℓ_τ, derived from the measurements are listed in Table 4 as absolute values and also as compared to characteristic lengths of the coronal plasma: $L_{\rm RTV}$, loop length expected for a standard hydrostatic loop model (e.g. Rosner et al. 1978, RTV hereafter) corresponding to the observed temperatures and densities, and the stellar radius $\rm R_\star$.

3. Discussion and conclusions

The discrepant O VIII and Ne X Lyα/Lyβ ratios found here for II Peg and IM Peg represent the first clear evidence of resonant scattering in coronal X-ray emission lines. The photon path lengths inferred from the observed ratios (Table 4) are:

1. about two orders of magnitude different from each other, reflecting the differences in the plasma densities found in Paper I for the characteristic temperatures of formation of the O VIII and Ne X lines respectively;
2. very small with respect to the stellar radius;
3. an order of magnitude larger than the loop lengths derived from RTV model scaling laws, for both hot and cooler plasma. In the ratio $\ell_\tau/L_{\rm RTV}$ the n_e terms cancel, so that this conclusion is completely independent of plasma density measurements.

We note that in the analysis performed in this paper processes of scattering of photons into the line-of-sight are not taken into account. The path lengths derived under this assumption should then be treated as lower limits. In the case of a uniform spherically-symmetric arrangement of emitting structures over the stellar surface, scattering into and out of the line-of-sight would be expected to compensate one another and yield no detectable effect. Therefore the detection of resonance scattering implies a non-uniform coronal distribution.

Assuming that the detected emission is mainly produced by loop-like emitting structures, as observed on the Sun, in order to be effective the scattering out of the line of sight would require a specific arrangement of the loops. The effectiveness of the scattering would be higher for loop axis lining up along the line of sight. We notice that the scattering process is isotropic, therefore while all the directions *out* of the line of sight are contributing to the decrease of the detected intensity, an increase on Lyα/Lyβ along the line of sight due to scattering of photons previously emitted in other directions *into* the line of sight is extremely unlikely because the direction of the line of sight is only one of the possible directions of the re-emitted photon.

Finally we note that in our analysis the findings of different optical depths in emitting regions on ostensibly similar active RS CVn-type binaries are puzzling. A possible explanation is that this is transient behaviour that might occur on all similarly active stars for a preferential arrangement of one or more coronal structures. We also note that, whereas both AR Lac and HR 1099 comprise

two late-type stars of more similar type, II Peg and IM Peg have unseen companions of unknown spectral type, though how this arrangement might benefit larger coronal photon path lengths is not obvious.

Acknowledgements

PT was partially supported by *Chandra* grants GO1-20006X and GO1-2012X under the SAO Predoctoral Fellowship program. JJD was supported by NASA contract NAS8-39073 to the *Chandra X-ray Center*; EED was supported by NASA grant NAG5-10872. GP and PT were partially supported by MIUR and by ASI.

References

Acton, L. W. 1978, ApJ, 225, 1069
Audard, M., Güdel, M., Sres, A., Raassen, A. J. J. & Mewe, R. 2003, A&A, 398, 1137
Beiersdorfer, P. 2003, ARA&A, 41, 343
Berdyugina, S. V., Jankov, S., Ilyin, I., Tuominen, I., Fekel, F. C. 1998, A&A, 334, 863
Berdyugina, S. V., Ilyin, I., Tuominen, I. 1999, A&A, 347, 932
Brickhouse, N. S., Dupree, A. K. & Young, P. R. 2001, ApJL, 562, L75
Chung, S. M., Drake, J. J., Kashyap, V. L., Lin, L., Ratzlaff, P. W. 2004, ApJ, 606, 1184
Doron, R. & Behar, E. 2002, ApJ, 574, 518
Drake, J. J. 2003, Advances in Space Research, 32, 945
Drake, J. J., Brickhouse, N. S., Kashyap, V., Laming, J. M., Huenemoerder, D. P., Smith, R., Wargelin, B. J. 2001, ApJL, 548, L81
Favata, F., Micela, G., Reale, F., Sciortino, S., & Schmitt, J. H. M. M. 2000, A&A, 362, 628
Gu, M. F. 2003, ApJ, 593, 1249
Huenemoerder, D. P., Canizares, C. R., Drake, J. J., Sanz-Forcada, J. 2003, ApJ, 595, 1131
Huenemoerder, D. P., Canizares, C. R., Schulz, N. S. 2001, ApJ, 559, 1135
Kaastra, J. S. & Mewe, R. 1995, A&A, 302, L13
Kastner, S. O. & Kastner, R. E. 1990, JQSRT, 44, 275
Kashyap, V. & Drake, J. J. 2000, Bull. Astron. Soc. India, 28, 475
Maggio, A., Pallavicini, R., Reale, F., & Tagliaferri, G. 2000, A&A, 356, 627
Marino, A., Micela, G., Peres, G., & Sciortino, S. 2003, A&A, 407, L63
Mazzotta, P., Mazzitelli, G., Colafrancesco, S. & Vittorio, N. 1998, A&AS, 133, 403
Mewe, R., Kaastra, J. S., van den Oord, G. H. J., Vink, J., Tawara, Y. 1997, A&A, 320, 147
Mitrou, C. K., Mathioudakis, M., Doyle, J. G. & Antonopoulou, E. 1997, A&A, 317, 776
Morton, D. C. 2003, ApJS, 149, 205
Ness, J.-U., Schmitt, J. H. M. M., Audard, M., Güdel, M., Mewe, R. 2003, A&A, 407, 347
Phillips, K. J. H., Mathioudakis, M., Huenemoerder, D. P., Williams, D. R., Phillips, M. E., Keenan, F. P. 2001, MNRAS, 325, 1500
Phillips, K. J. H., Greer, C. J., Bathia, A. K., Coffey, I. H., Barnsley, R. & Keenan, F. P. 1997, A&A, 324, 381
Phillips, K. J. H., Greer, C. J., Bathia, A. K. & Keenan, F. P. 1996, ApJL, 469, L57
Raassen, A. J. J. et al. 2002, A&A, 389, 228
Reale, F., Güdel, M., Peres, G., & Audard, M. 2004, A&A, 416, 733
Redfield, S., Ayres, T. R., Linsky, J. L., Ake, T. B., Dupree, A. K., Robinson, R. D., Young, P. R. 2003, ApJ, 585, 993
Rosner, R., Tucker, W. H. & Vaiana, G. S. 1978, ApJ, 220, 643
Saba, J. L. R., Schmelz, J. T., Bathia, A. K. & Strong, K. T. 1999, ApJ, 510, 1064
Schmelz, J. T., Saba, J. L. R., Chauvin, J. C. & Strong, K. T. 1997, ApJ, 477, 509
Schmitt, J. H. M. M. & Favata, F. 1999, Nature, 401, 44
Smith, R. K., Brickhouse, N. S., Liedahl, D. A. & Raymond, J. C. 2001, ApJL, 556, L91
Strassmeier, K. G., Hall, D. S., Fekel, F. C. & Scheck, M. 1993, A&AS, 100, 173
Testa, P., Drake, J. J., Peres, G. & DeLuca, E. E. 2004, ApJL, 609, L79
Testa, P., Drake, J. J. & Peres, G. 2004, ApJ, in press